Supplementary Material (ESI) for CrystEngComm

Three new inorganic-organic hybrid compounds constructed from two kinds of octamolybdate clusters and flexible multidentate N-donor ligand: syntheses, structures, electrochemistry, luminescence, and photocatalytic properties

Wei Wang, Jin Yang,* Wei-Qiu Kan, and Jian-Fang Ma*

Key Lab of Polyoxometalate Science, Department of Chemistry, Northeast Normal University, Changchun 130024, People's Republic of China

* Correspondence authors

E-mail: yangjinnenu@yahoo.com.cn (J. Yang)

E-mail: majf247@sohu.com (J.-F. Ma)

Fax: +86-431-85098620 (J.-F. Ma)

Table S1. Selected bond distances (Å) and angles (°) for **1**.

Zn(1)-N(9)#1	2.079(7)	Zn(1)-O(1W)	2.109(6)
Zn(1)-N(6)	2.142(6)	Zn(1)-O(7)	2.145(5)
Zn(1)-N(3)#2	2.151(6)	Zn(1)-N(15)	2.168(7)
Zn(2)-O(4W)	1.86(5)	Zn(2)-O(6W)	1.93(2)
Zn(2)-O(8W)	2.066(14)	Zn(2)-N(14)	2.079(8)
Zn(2)-N(5)	2.092(7)	Zn(2)-O(3W)	2.095(19)
Zn(2)-O(7W)	2.14(4)	Zn(2)-N(2)#2	2.155(7)
Zn(2)-O(2W)	2.19(2)	N(9)#1-Zn(1)-O(1W)	89.5(3)
N(9)#1-Zn(1)-N(6)	174.2(3)	O(1W)-Zn(1)-N(6)	85.1(2)
N(9)#1-Zn(1)-O(7)	94.2(2)	O(1W)-Zn(1)-O(7)	87.0(2)
N(6)-Zn(1)-O(7)	87.6(2)	N(9)#1-Zn(1)-N(3)#2	96.8(2)
O(1W)-Zn(1)-N(3)#2	171.4(2)	N(6)-Zn(1)-N(3)#2	88.9(2)
O(7)-Zn(1)-N(3)#2	86.7(2)	N(9)#1-Zn(1)-N(15)	89.2(3)
O(1W)-Zn(1)-N(15)	91.4(3)	N(6)-Zn(1)-N(15)	88.9(3)
O(7)-Zn(1)-N(15)	176.3(2)	N(3)#2-Zn(1)-N(15)	94.6(3)
O(4W)-Zn(2)-O(6W)	88.6(15)	O(4W)-Zn(2)-O(8W)	69.8(17)
O(6W)-Zn(2)-O(8W)	71.8(9)	O(4W)-Zn(2)-N(14)	112.5(18)
O(6W)-Zn(2)-N(14)	91.1(8)	O(8W)-Zn(2)-N(14)	162.9(5)
O(4W)-Zn(2)-N(5)	85.1(14)	O(6W)-Zn(2)-N(5)	173.4(7)
O(8W)-Zn(2)-N(5)	104.0(5)	N(14)-Zn(2)-N(5)	93.1(3)
O(4W)-Zn(2)-O(3W)	30.6(17)	O(6W)-Zn(2)-O(3W)	72.9(9)
O(8W)-Zn(2)-O(3W)	90.1(7)	N(14)-Zn(2)-O(3W)	86.3(6)
N(5)-Zn(2)-O(3W)	102.3(6)	O(4W)-Zn(2)-O(7W)	57(2)

O(6W)-Zn(2)-O(7W)	84.6(12)	O(8W)-Zn(2)-O(7W)	17.1(8)
N(14)-Zn(2)-O(7W)	169.1(10)	N(5)-Zn(2)-O(7W)	90.4(9)
O(3W)-Zn(2)-O(7W)	82.8(11)	O(4W)-Zn(2)-N(2)#2	148.8(18)
O(6W)-Zn(2)-N(2)#2	95.8(7)	O(8W)-Zn(2)-N(2)#2	82.2(4)
N(14)-Zn(2)-N(2)#2	98.3(3)	N(5)-Zn(2)-N(2)#2	88.6(2)
O(3W)-Zn(2)-N(2)#2	167.9(6)	O(7W)-Zn(2)-N(2)#2	92.1(10)
O(4W)-Zn(2)-O(2W)	25.8(17)	O(6W)-Zn(2)-O(2W)	86.9(10)
O(8W)-Zn(2)-O(2W)	93.7(8)	N(14)-Zn(2)-O(2W)	86.9(7)
N(5)-Zn(2)-O(2W)	88.3(8)	O(3W)-Zn(2)-O(2W)	14.0(7)
O(7W)-Zn(2)-O(2W)	82.9(12)	N(2)#2-Zn(2)-O(2W)	174.1(7)

Symmetry transformations used to generate equivalent atoms: $^{\#1}$ -x + 1, -y - 1, -z + 1; $^{\#2}$ x + 1, y, z; $^{\#3}$ -x + 1, -y - 2, -z + 1; $^{\#4}$ -x, -y - 2, -z + 1; $^{\#5}$ -x + 2, -y, -z; $^{\#6}$ x - 1, y, z.

Table S2. Selected bond distances (Å) and angles (°) for **2**.

Zn(1)-O(34)	2.014(16)	Zn(1)-N(11)#1	2.03(7)
Zn(1)-O(3W)	2.106(10)	Zn(1)-N(2)#2	2.123(9)
Zn(1)-N(9)	2.22(4)	Zn(1)-O(12)#3	2.245(7)
Zn(2)-O(30)#4	1.940(8)	Zn(2)-O(2W)	1.992(17)
Zn(2)-N(8)	2.046(12)	Zn(2)-O(33)	2.00(2)
Zn(2)-N(12)#1	2.13(8)	Zn(3)-O(13)#6	2.271(7)
Zn(3)-N(5)	2.024(9)	Zn(3)-N(17)#5	2.079(8)
Zn(3)-O(1W)	2.092(9)	Zn(3)-O(16)	2.142(7)
Zn(3)-O(18)	2.250(8)	O(34)-Zn(1)-N(11)#1	100(2)
N(11)#1-Zn(1)-O(3W)	167(2)	O(34)-Zn(1)-O(3W)	93.7(5)

O(34)-Zn(1)-N(2)#2	97.0(5)	N(11)#1-Zn(1)-N(2)#2	88(2)
O(3W)-Zn(1)-N(2)#2	91.3(4)	O(34)-Zn(1)-N(9)	103.3(12)
N(11)#1-Zn(1)-N(9)	80(2)	O(3W)-Zn(1)-N(9)	95.9(11)
N(2)#2-Zn(1)-N(9)	157.9(11)	O(34)-Zn(1)-O(12)#3	173.8(5)
N(11)#1-Zn(1)-O(12)#3	84(2)	O(3W)-Zn(1)-O(12)#3	82.8(3)
N(2)#2-Zn(1)-O(12)#3	77.9(3)	N(9)-Zn(1)-O(12)#3	82.3(11)
O(30)#4-Zn(2)-O(2W)	100.1(6)	O(30)#4-Zn(2)-O(33)	113.0(7)
O(2W)-Zn(2)-O(33)	82.6(8)	O(30)#4-Zn(2)-N(8)	109.6(4)
O(2W)-Zn(2)-N(8)	99.1(7)	O(33)-Zn(2)-N(8)	136.3(7)
O(30)#4-Zn(2)-N(12)#1	96(2)	O(2W)-Zn(2)-N(12)#1	161(2)
O(33)-Zn(2)-N(12)#1	82.1(18)	N(8)-Zn(2)-N(12)#1	84.4(18)
N(5)-Zn(3)-N(17)#5	164.2(4)	N(5)-Zn(3)-O(1W)	92.7(4)
N(17)#5-Zn(3)-O(1W)	96.1(3)	N(5)-Zn(3)-O(16)	101.5(4)
N(17)#5-Zn(3)-O(16)	92.3(3)	O(1W)-Zn(3)-O(16)	84.7(3)
N(5)-Zn(3)-O(18)	88.4(3)	N(17)#5-Zn(3)-O(18)	78.9(3)
O(1W)-Zn(3)-O(18)	87.8(3)	O(16)-Zn(3)-O(18)	167.8(3)
N(5)-Zn(3)-O(13)#6	91.2(4)	N(17)#5-Zn(3)-O(13)#6	81.2(3)
O(1W)-Zn(3)-O(13)#6	173.7(3)	O(16)-Zn(3)-O(13)#6	89.6(3)
O(18)-Zn(3)-O(13)#6	97.3(3)		

Symmetry transformations used to generate equivalent atoms: #1 -x + 2, -y + 2, -z + 1; #2 -x + 1, -y + 1, -z; #3 -x + 1, -y, -z; #4 -x + 2, -y + 1, -z + 1; #5 -x + 1, -y, -z + 1; #6 -x + 1, -y - 1, -z; #7 x, y - 1, z; #8 x, y + 1, z.

Table S3. Selected bond distances (Å) and angles (°) for **3**.

Cd(1)-N(15)	2.226(7)	Cd(1)-O(22)	2.272(6)

Cd(1)-N(9)#1	2.292(7)	Cd(1)-O(21)	2.306(6)
Cd(1)-O(8)	2.320(6)	Cd(1)-O(3W)	2.336(7)
Cd(2)-O(1W)	2.108(9)	Cd(2)-N(3)#2	2.301(14)
Cd(2)-N(6)#2	2.315(14)	Cd(2)-N(12)#3	2.332(9)
Cd(2)-O(2W)	2.334(17)	Cd(2)-O(33)	2.337(7)
N(15)-Cd(1)-O(22)	95.5(3)	N(15)-Cd(1)-N(9)#1	170.2(3)
O(22)-Cd(1)-N(9)#1	93.9(3)	N(15)-Cd(1)-O(21)	96.7(3)
O(22)-Cd(1)-O(21)	91.7(2)	N(9)#1-Cd(1)-O(21)	80.1(3)
N(15)-Cd(1)-O(8)	95.5(2)	O(22)-Cd(1)-O(8)	165.7(2)
N(9)#1-Cd(1)-O(8)	75.6(2)	O(21)-Cd(1)-O(8)	95.9(2)
N(15)-Cd(1)-O(3W)	92.1(3)	O(22)-Cd(1)-O(3W)	82.6(2)
N(9)#1-Cd(1)-O(3W)	91.9(3)	O(21)-Cd(1)-O(3W)	169.9(2)
O(8)-Cd(1)-O(3W)	88.1(2)	O(1W)-Cd(2)-N(3)#2	179.1(6)
O(1W)-Cd(2)-N(6)#2	99.0(7)	N(3)#2-Cd(2)-N(6)#2	81.8(6)
O(1W)-Cd(2)-N(12)#3	85.8(6)	N(3)#2-Cd(2)-N(12)#3	94.6(4)
N(6)#2-Cd(2)-N(12)#3	93.7(4)	O(1W)-Cd(2)-O(2W)	90.9(7)
N(3)#2-Cd(2)-O(2W)	88.6(5)	N(6)#2-Cd(2)-O(2W)	94.9(6)
N(12)#3-Cd(2)-O(2W)	171.2(5)	O(1W)-Cd(2)-O(33)	89.8(6)
N(3)#2-Cd(2)-O(33)	89.5(4)	N(6)#2-Cd(2)-O(33)	165.0(5)
N(12)#3-Cd(2)-O(33)	74.7(3)	O(2W)-Cd(2)-O(33)	97.2(4)

Symmetry transformations used to generate equivalent atoms: $^{\#1}$ -x + 2, -y, -z + 1; $^{\#2}$ -x + 1, -y, -z; $^{\#3}$ -x + 2, -y + 1, -z + 1; $^{\#4}$ -x + 2, -y + 1, -z + 2; $^{\#5}$ -x + 1, -y, -z + 1.

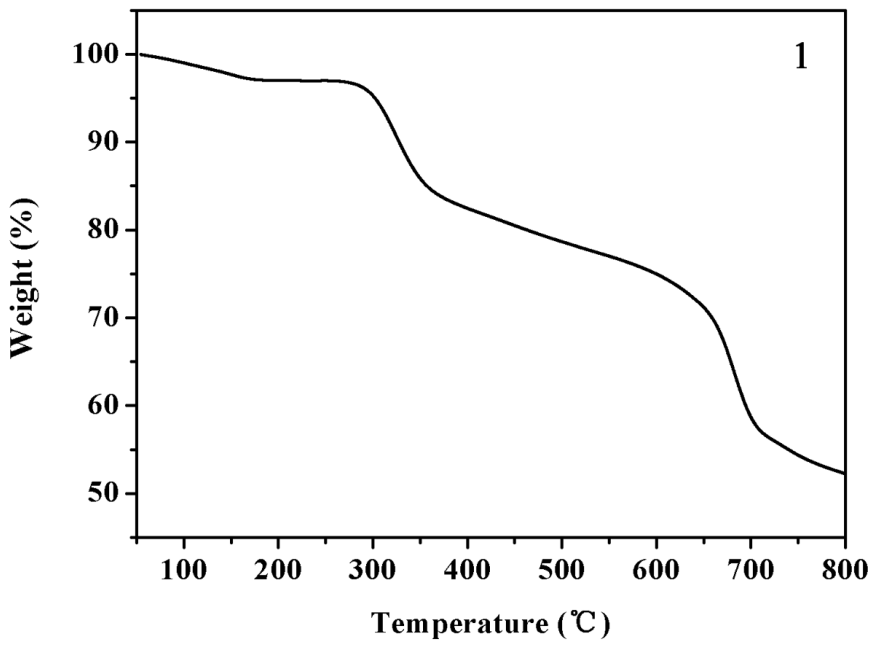

Fig. S1 TGA curve of compound **1**. The weight loss of 2.8% from 50 to 165 °C is attributed to the loss of seven water molecule (calcd 3.2%).

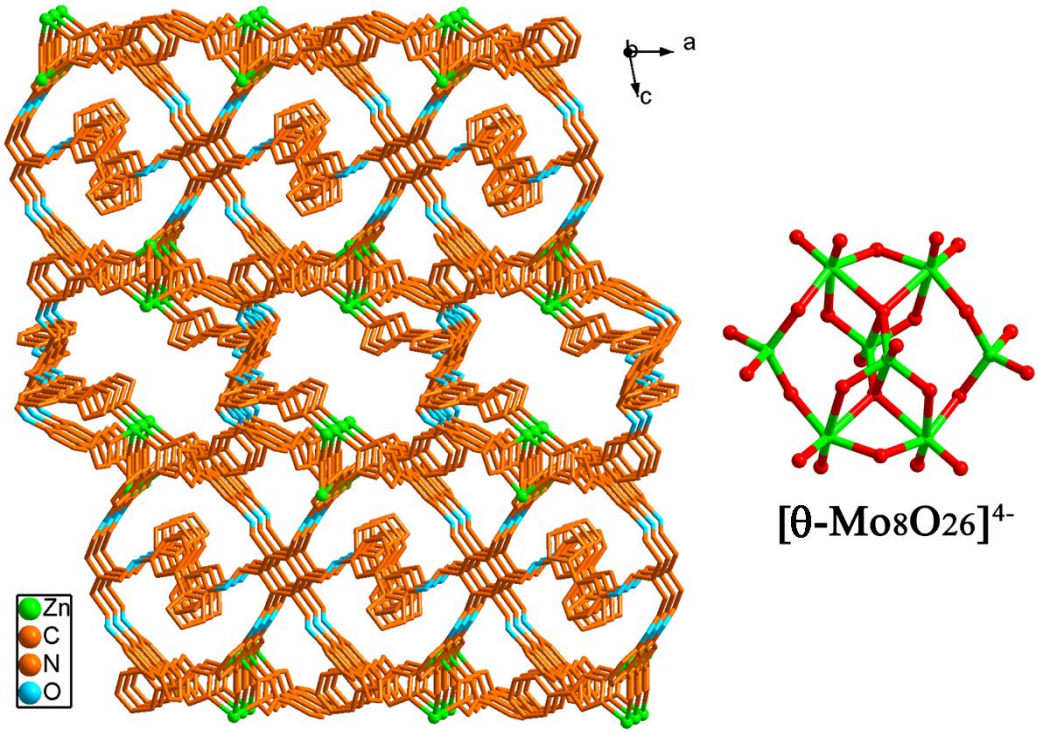

Fig. S2 The Zn-organic framework constructed by the Zn(II) ions and the htpmb ligands as well as the structure of $[\theta\text{-}Mo_8O_{26}]^{4-}$ anion.

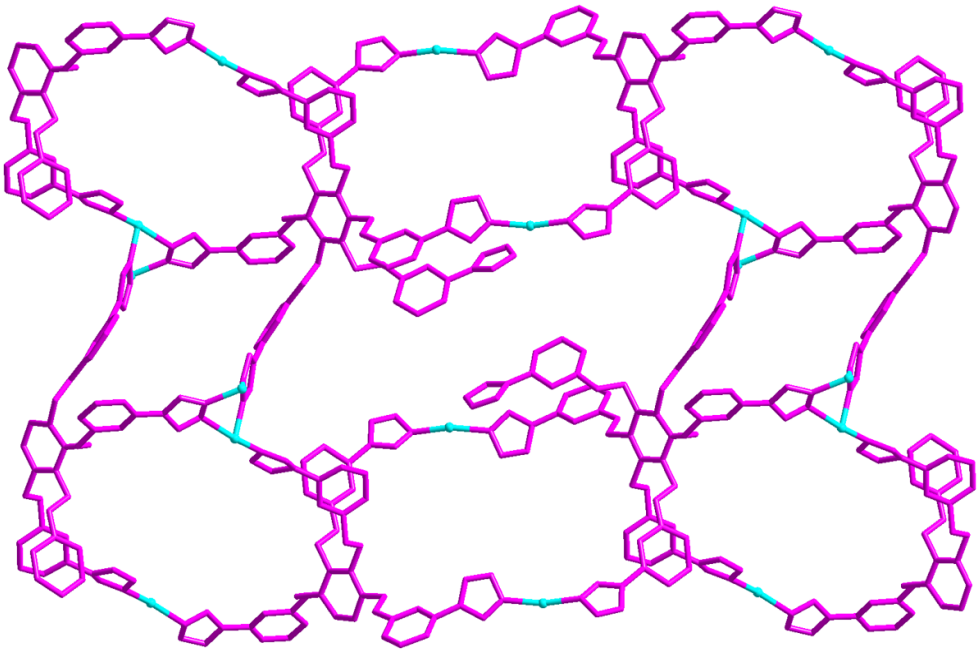

(a)

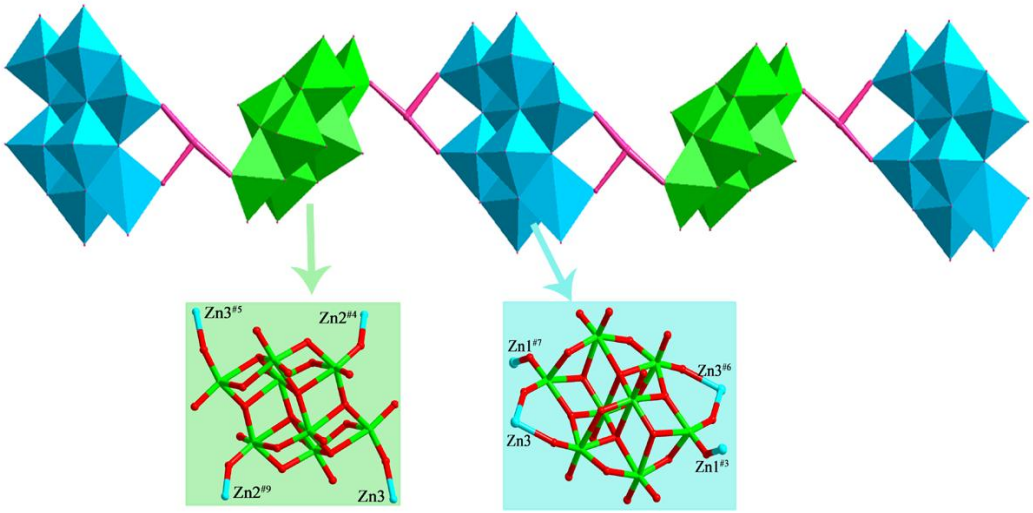

(b)

Fig. S3 (a) The 2D layer constructed by the Zn(II) ions and the htpmb ligands. (b) The 1D infinite chain constructed by the Zn3 ions and the $[\gamma\text{-}Mo_8O_{26}]^{4-}$ anions.

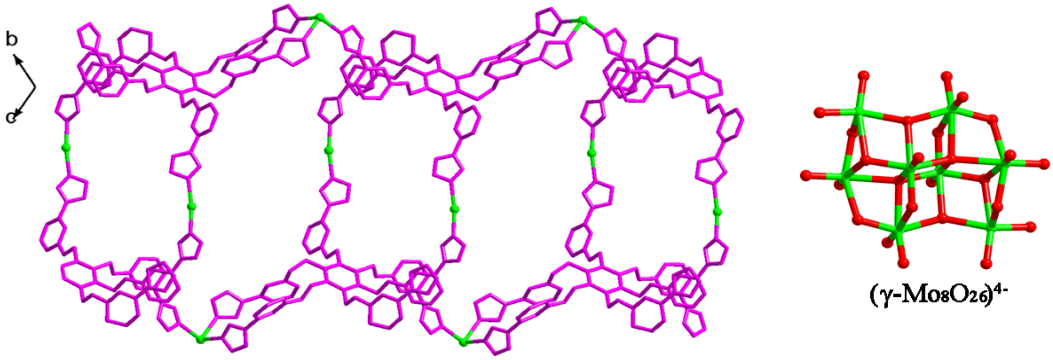

Fig. S4 The Cd-organic chain constructed by the Cd(II) ions and the htpmb ligands as well as the structure of $[\gamma\text{-}Mo_8O_{26}]^{4-}$ anion.

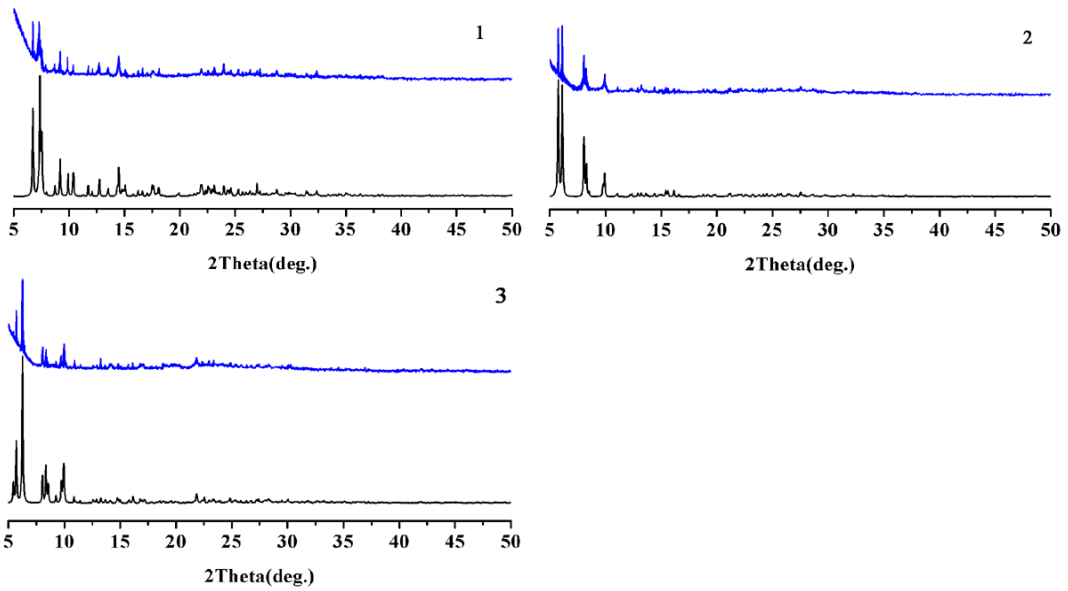

Fig. S5 The simulated (black) PXRD patterns of compounds **1-3** and the PXRD patterns of compounds **1-3** after photocatalytic processes (blue).

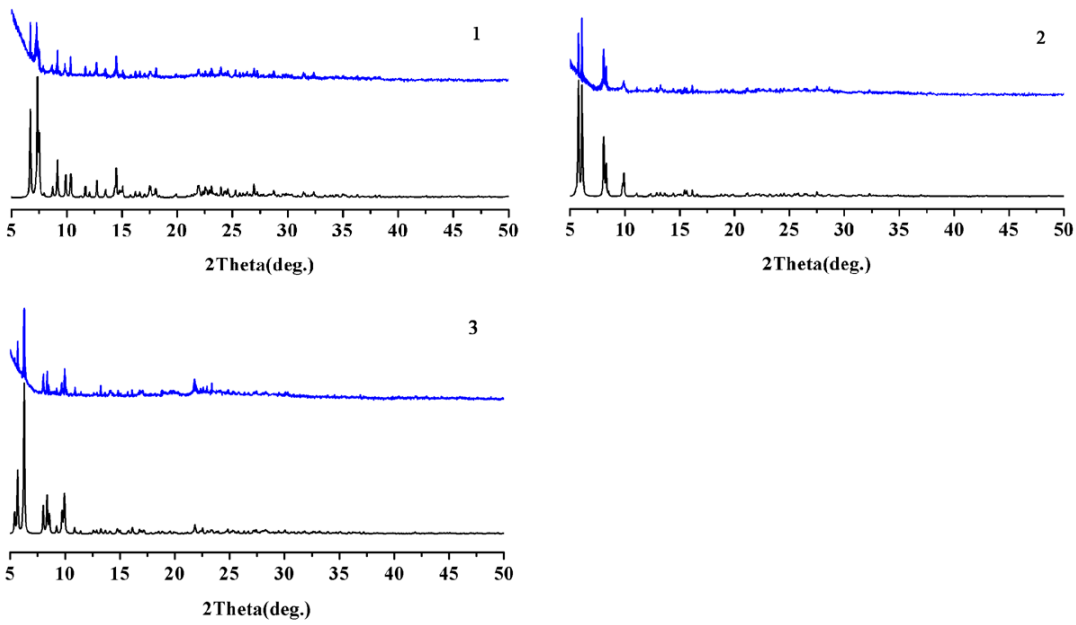

Fig. S6 Simulated (black) and experimental (blue) PXRD patterns of **1-3**.

UV-vis spectra and optical band gaps.

The UV-vis absorption spectra of compounds **1**–**3** were performed in the crystalline state at room temperature (Fig. S7). The energy bands from 220 to 275 nm for **1**–**3** may be assigned to the O → Mo charge transfer transitions.[1] Some octamolybdate-based inorganic-organic hybrid materials have been proven to be potential semiconductors.[2] Therefore, we studied the conductivities of compounds **1**–**3**. The measurements of diffuse reflectivity for powder samples of **1- 3** have been carried out to obtain their band gaps (Eg). The E_g values are defined as the intersection point between the energy axis and the line extrapolated from the linear portion of the adsorption edge in the plot of the Kubelka-Munk function F versus energy E.[3] As illustrated in Fig. S8, the E_g values of **1**–**3** are 2.63, 3.33, and 3.20 eV, respectively. The optical band gaps indicate that compounds **1**–**3** may be underlying semi-conducting materials.

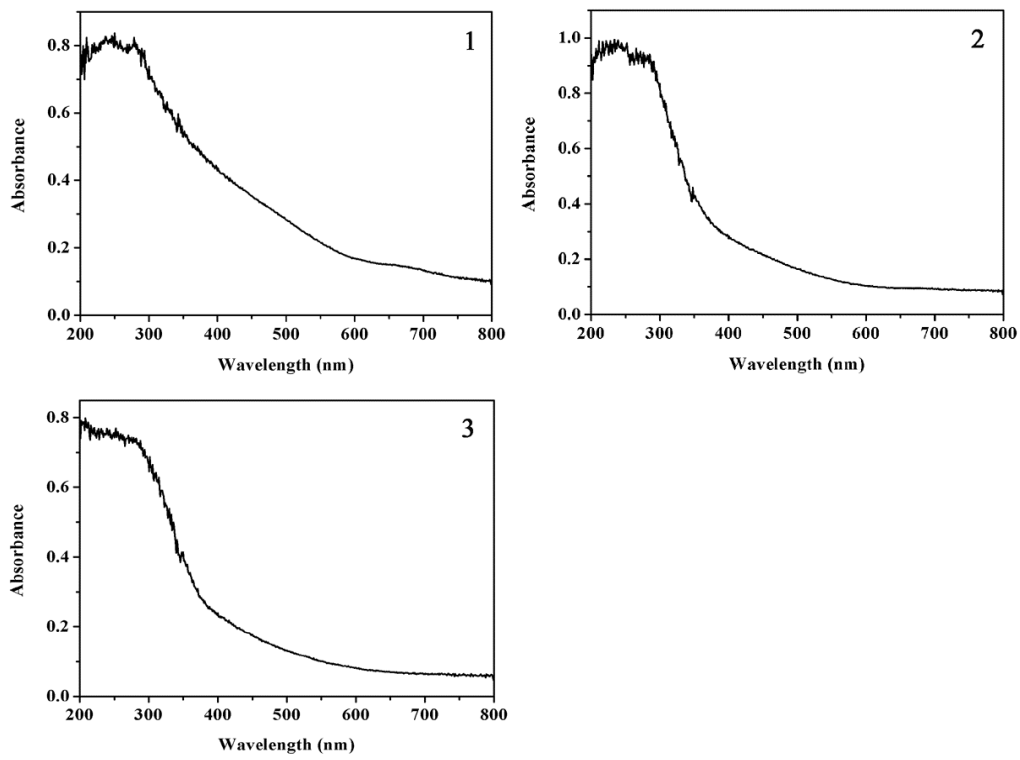

Fig. S7 UV-vis absorption spectra of compounds **1-3**.

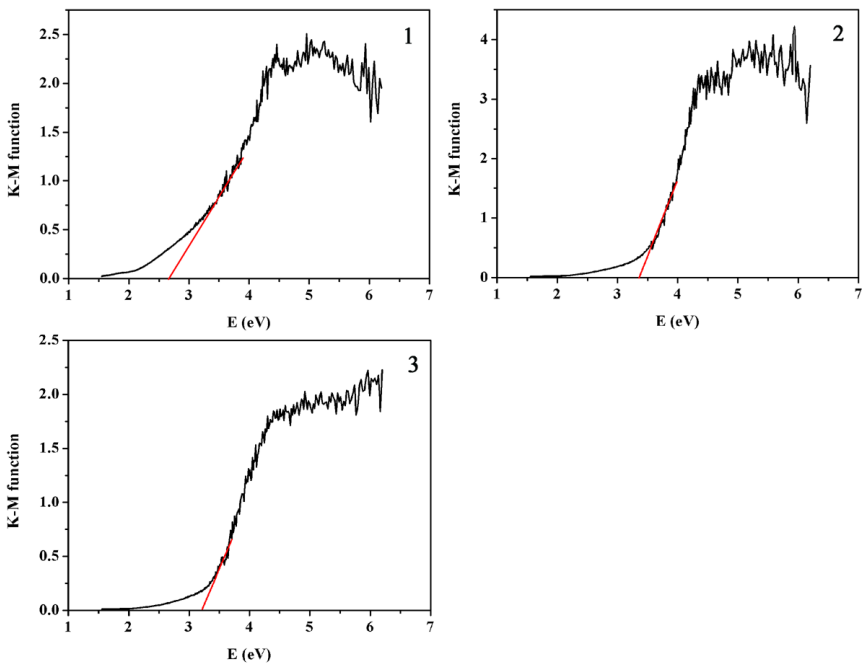

Fig. S8 UV-Vis-NIR diffuse reflectance spectra of K-M functions *vs* energy (eV) of the compounds **1**–**3**.

Luminescent properties

The luminescent properties of inorganic-organic hybrid compounds have attracted a great deal of interest due to their various applications in chemical sensors, photochemistry, and electroluminescent displays.[2a,4,5] Therefore, in this work, the luminescent properties of htpmb ligand and compounds **1**–**3** were studied in the solid state at room temperature. The emission and excitation peaks of the htpmb ligand and compounds **1**–**3** are illustrated in Fig. S9.

The free htpmb ligand shows emission peak at 480 nm (λ_{ex} = 345 nm). This emission may be assigned to the $\pi^* \rightarrow n$ or $\pi^* \rightarrow \pi$ transition.[6] The emission spectra of the compounds **1-3** exhibit the main peaks at 430 nm for **1** (λ_{ex} = 302 nm), 460 nm for **2** (λ_{ex} = 300 nm), and 371 nm for **3** (λ_{ex} = 260 nm). Compared with the free htpmb ligand, the main emission peaks of compounds **1**–**3** are blue-shifted to different extents. The observed blue-shifts may be attributed to the following factors: (1) there may exist L → M charge-transfer transitions between htpmb ligands and molybdenum atoms; (2) htpmb ligands may change their highest occupied molecular orbital (HOMO) and lowest occupied molecular orbital (LUMO) energy levels after

coordinating to metal ions.[2b]

The luminescence decay curves of compounds **1-3** at room temperature (Fig. S10) fit well into a double-exponential function as $I = A + B1 \times \exp(-t/\tau_1) + B2 \times \exp(-t/\tau_2)$. The emission decay lifetimes of **1-3** are τ_1 = 1.16 μs (22.31%) and τ_2 = 8.76 μs (77.69%) (χ^2 = 1.009) for **1**, τ_1 = 2.93 μs (21.28%) and τ_2 = 9.56 μs (78.72%) (χ^2 = 1.010) for **2**, and τ_1 = 0.66 μs (48.44%) and τ_2 = 6.41 μs (51.56%) (χ^2 = 1.015) for **3**. The luminescence lifetimes of **1-3** are shorter than the ones from a triplet state (>10^{-3} s), so the emissions should arise from the singlet state.

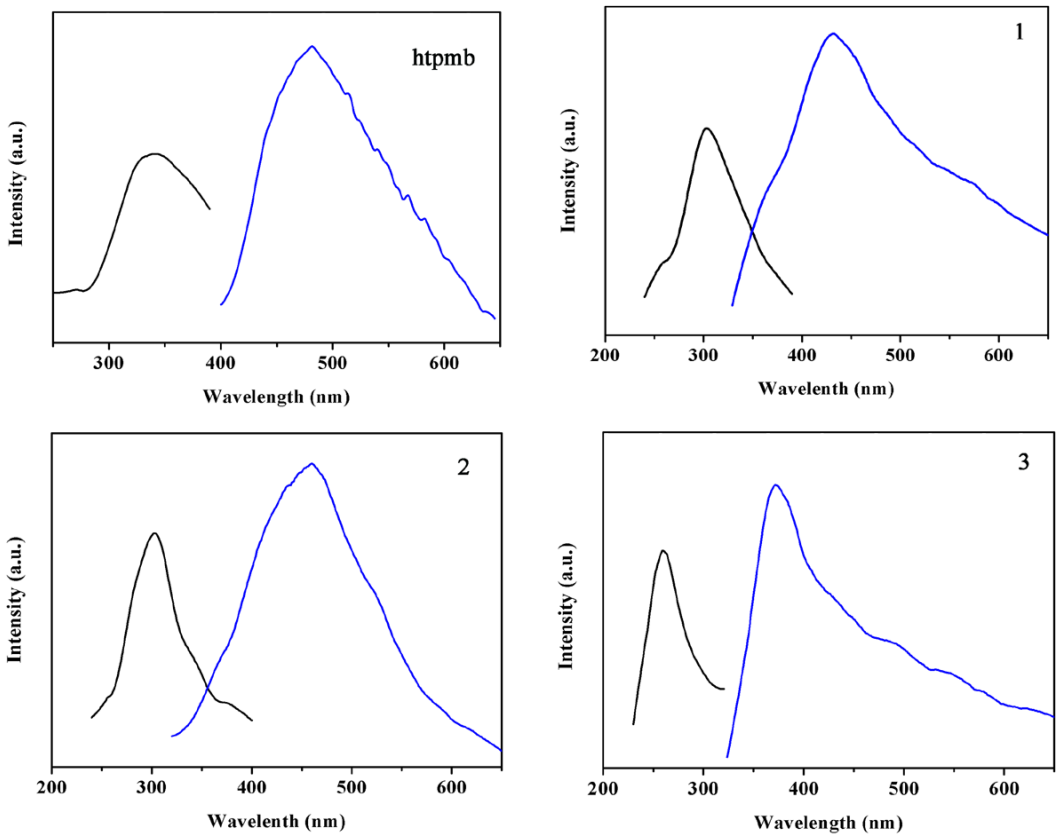

Fig. S9 Solid-state excitation and emission spectra of the htpmb ligand and compounds **1-3** at room temperature.

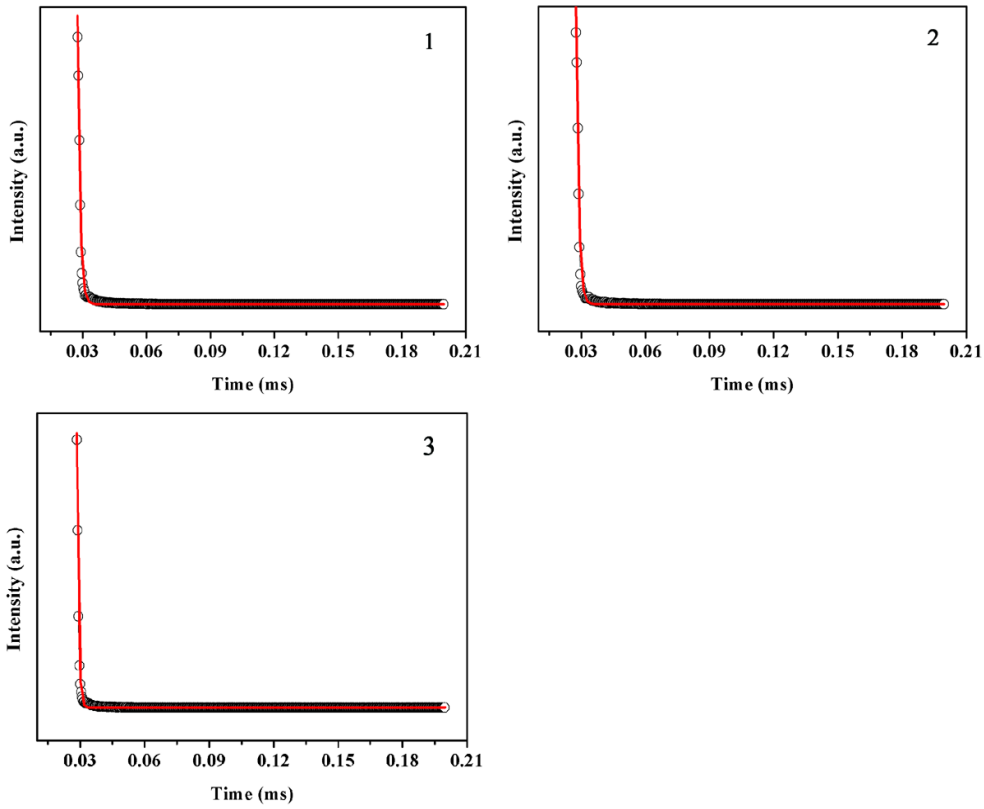

Fig. S10 Luminescence decay curves for compounds **1-3** (the black circles represent experimental data, and the solid red lines represent fitting results).

References

1 Y. Xia, P. F. Wu, Y. G. Wei, Y. Wang and H. Y. Guo, *Cryst. Growth Des.*, 2006, **6**, 253.

2 (*a*) W. Q. Kan, J. Yang, Y.-Y. Liu and J.-F. Ma, *Inorg. Chem.*, 2012, **51**, 11266; (*b*) H.-Y. Liu, B. Liu, J. Yang, Y.-Y. Liu, J.-F. Ma and H. Wu, *Dalton Trans.*, 2011, **40**, 9782.

3 (*a*) W. M. Wesley and W. G. H. Harry, *Reflectance Spectroscopy*, Wiley, New York, 1966; (*b*) J. I. Pankove, *Optical Processes in Semiconductors*, Prentice Hall, Englewood Cliffs, NJ, 1971.

4 A. Dolbecq, E. Dumas, C. R. Mayer and P. Mialane, *Chem. Rev.*, 2010, **110**, 6009.

5 (*a*) K. Yu, B. Wan, Y. Yu, L. Wang, Z.-H. Su, C.-M. Wang, C.-X. Wang and B. B. Zhou, *Inorg. Chem.*, 2013, **52**, 485; (*b*) Y. J. Cui, Y. F. Yue, G. D. Qian and B. L. Chen, *Chem. Rev.*, 2012, **112**, 1126; (*c*) N. Stock and S. Biswas, *Chem. Rev.*, 2012,

112, 933.

6 (*a*) H. Y. Bai, J.-F. Ma, J. Yang, Y. Y. Liu, H. Wu and J. C. Ma, *Cryst. Growth Des*., 2010, **10**, 995; (*b*) K. H. He, Y. W. Li, Y. Q. Chen, W. C. Song and X. H. Bu, *Cryst. Growth Des.*, 2012, **12**, 27; (*c*) L. P. Zhang, J. F. Ma, J. Yang, Y. Y. Pang and J. C. Ma, *Inorg. Chem.*, 2010, **49**, 1535.